AGU PUBLICATIONS

Geophysical Research Letters

RESEARCH LETTER
10.1002/2015GL063272

Key Points:
- Energy is rapidly supplied to Jovian aurora during the solar wind quiet period
- Auroral morphology suggests a global change in the auroral process
- This suggests an internally driven disturbance during the quiet period

Correspondence to:
T. Kimura,
kimura@stp.isas.jaxa.jp

Citation:
Kimura, T., et al. (2015), Transient internally driven aurora at Jupiter discovered by Hisaki and the Hubble Space Telescope, *Geophys. Res. Lett.*, *42*, 1662–1668, doi:10.1002/2015GL063272.

Received 27 JAN 2015
Accepted 18 FEB 2015
Accepted article online 20 FEB 2015
Published online 25 MAR 2015

Transient internally driven aurora at Jupiter discovered by Hisaki and the Hubble Space Telescope

T. Kimura[1], S. V. Badman[2], C. Tao[3], K. Yoshioka[1], G. Murakami[1], A. Yamazaki[1], F. Tsuchiya[4], B. Bonfond[5], A. J. Steffl[6], A. Masters[1,7], S. Kasahara[1], H. Hasegawa[1], I. Yoshikawa[8,9], M. Fujimoto[1,10], and J. T. Clarke[11]

[1]Institute of Space and Astronautical Science, Japan Aerospace Exploration Agency, Sagamihara, Japan, [2]Department of Physics, Lancaster University, Lancaster, UK, [3]Institut de Recherche en Astrophysique et Planétologie, Université de Toulouse, CNRS, Toulouse, France, [4]Planetary Plasma and Atmospheric Research Center, Tohoku University, Sendai, Japan, [5]Laboratoire de Physique Atmosphérique et Planétaire, Université de Liège, Liège, Belgium, [6]Department of Space Studies, Southwest Research Institute, Boulder, Colorado, USA, [7]Space and Atmospheric Physics, Imperial College London, London, UK, [8]Department of Earth and Planetary Science, Graduate School of Science, University of Tokyo, Tokyo, Japan, [9]Department of Complexity Science and Engineering, The University of Tokyo, Chiba, Japan, [10]Earth-Life Science Institute, Tokyo Institute of Technology, Tokyo, Japan, [11]Center for Space Physics, Boston University, Boston, Massachusetts, USA

Abstract Jupiter's auroral emissions reveal energy transport and dissipation through the planet's giant magnetosphere. While the main auroral emission is internally driven by planetary rotation in the steady state, transient brightenings are generally thought to be triggered by compression by the external solar wind. Here we present evidence provided by the new Hisaki spacecraft and the Hubble Space Telescope that shows that such brightening of Jupiter's aurora can in fact be internally driven. The brightening has an excess power up to ~550 GW. Intense emission appears from the polar cap region down to latitudes around Io's footprint aurora, suggesting a rapid energy input into the polar region by the internal plasma circulation process.

1. Introduction

Jupiter's main auroral emission is basically driven by electrical currents acting to spin-up magnetospheric plasma which has fallen behind corotation with the planet. This is the most steady component of the auroral emission, although all the auroral features exhibit temporal variability on time scales from a few minutes to 100 days. Two causes of the temporal variability in the auroral emissions and other magnetospheric processes have been proposed from previous studies [e.g., *Grodent*, 2014, and the references therein]: compression of the magnetosphere by interplanetary shocks [*Cowley and Bunce*, 2003a, 2003b; *Cowley et al*., 2007; *Yates et al*., 2014] and changes in the mass loading and radial plasma transport on closed field lines [*Hill*, 2001; *Nichols and Cowley*, 2003; *Nichols*, 2011]. Many recent observations indicated responses of transient auroral emission to the arrival of interplanetary shocks [e.g., *Baron et al*., 1996; *Waite et al*., 2001; *Prangé et al*., 2001, 2004; *Gurnett et al*., 2002; *Nichols et al*., 2007; *Clarke et al*., 2009; *Tsuchiya et al*., 2010].

Especially for the low-latitude aurora and main oval, which map to the inner and middle magnetosphere, the mass loading and radial plasma transport are believed to play a more significant role in the auroral process than the external solar wind, because of Jupiter's fast rotation and large plasma supply from Io [*Vasyliūnas*, 1983; *Khurana et al*., 2004; *Krupp et al*., 2004]. The temporal variability of Jupiter's auroral emission has been observed mainly in ultraviolet (UV) wavelengths by the International Ultraviolet Explorer (IUE), Hubble Space Telescope (HST), and the Cassini spacecraft. IUE continuously monitored the far ultraviolet (FUV) spectral ratio through 1 month [*Prangé et al*., 2001]. The monitoring indicated short- and long-term variability in the FUV aurora from 5 h to 5–10 days which is suggestive of recurrent energy release in Jupiter's magnetosphere. Long-term observations by HST and Cassini detected solar wind-driven variability in auroral brightness and morphology on time scales of a few days or longer [e.g., *Pryor et al*., 2005; *Nichols et al*., 2007, 2009; *Clarke et al*., 2009]. However, some HST images indicated activity uncorrelated with the solar wind [*Nichols et al*., 2009; *Clarke et al*., 2009], which were interpreted as internally driven auroras associated with the mass loading and related plasma circulation [*Bonfond et al*., 2012]. Gradual mass loading from Io and related plasma circulation inside Jupiter's magnetosphere over time scales of 100 days are suggested to internally trigger a progressive expansion of the main emissions and an increased occurrence of bright low-latitude emissions

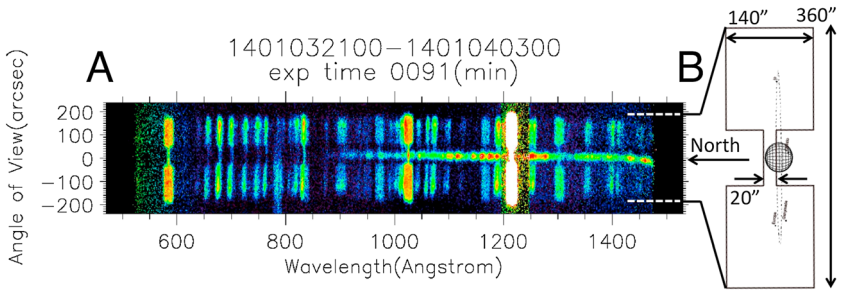

Figure 1. (a) Imaging spectrum observed by EXCEED spectrometer from 21:00 day 3 to 03:00 day 4 with an exposure time of 91 min. Color indicates arbitrary intensity of the imaging spectrum. (b) Geometrical relation of the slit with respect to the planet. The planetary disk is modeled by http://pds-rings.seti.org/tools/viewer2_jup.html. The dumbbell-shaped slit is centered at Jupiter's northern aurora aligned with the equator. The narrow region with a width of 20 arcsec covers the northern polar region, whereas the wide region of 140 arcsec covers the dawn and dusk ansae of Io plasma torus. Dotted line indicates Io's orbit.

[*Bonfond et al*., 2012]. More rapid internally driven variations of the auroral emissions have also been observed in the radio hectometric emissions [*Yoneda et al*., 2013].

The long-term continuous monitoring of aurora has not been made in comparison with auroral morphologies and solar wind variations. The early monitoring by IUE provided the spectral ratio with a 45–60 min resolution without morphology and solar wind information [*Prangé et al*., 2001]. On the other hand, HST provides highly resolved imaging or spectra with a few exposures of 100 s during 45 min visibility time of Jupiter every 96 min orbital period [e.g., *Clarke et al*., 2009]. Cassini's UV spectrometer had a duty cycle at Jupiter of observations with ~10 h duration every ~20 h [*Pryor et al*., 2005]. These observations have not simultaneously resolved hour-to-hour variability and spatial structure which are likely associated with onset time of energy release and transfer path of released energy.

Here we report the internally driven aurora discovered from the quasi-continuous monitoring of the extreme ultraviolet (EUV) auroral intensity made by the EUV spectrometer Extreme ultraviolet spetrosCope for ExosphEric Dynamics (EXCEED) [*Yoshioka et al*., 2013] on board the Earth-orbiting Hisaki satellite [*Nakaya et al*., 2012]. The observations were made at 10 min resolution for 40 min out of every 100 min Hisaki orbit over 2 months from late 2013 to early 2014. The continuous monitoring is compared with the highly resolved auroral imaging by HST and solar wind variations at Jupiter extrapolated from Earth's orbit.

2. Data Set

EUV photons measured by EXCEED are reduced to spatio-spectral images with 1024 × 1024 pixels in this study. The spectral range spans from 470 to 1530 Å with a resolution of 3 Å full width at half maximum. The angle of view ranges from −180 to +180 arcsec from the light axis with a spatial pixel size of 4.1 arcsec and pointing accuracy of ±2 arcsec. The dumbbell-shaped slit with a width of 140 arcsec was used for observation of Jupiter during the observation period of the present study. The imaging spectra are acquired continuously during 40 min of every 100 min Hisaki orbit. Figure 1 indicates an example of imaging spectrum measured during the present analysis period.

The total energy flux of EUV photons is reduced from integration of 10 min resolution imaging spectra over 900–1480 Å. The auroral energy flux is extracted from the direction within 20 arcsec from Jupiter's north pole. The total emitted power is derived by integration of the total energy flux through 4π steradian assuming isotropic directivity of auroral emission. The exposure is suspended when Jupiter is eclipsed by the Earth and when Hisaki flew through the Southern Atlantic Anomaly. Geocoronal emission lines at 1025 Å (H-Lyman β), 1168 Å neutral atomic nitrogen N(I), 1216 Å (H-Lyman α), 1304 Å neutral atomic oxygen O(I), and 1356 Å (OI) are ignored in the photon integration.

The auroral total power is contaminated by the disk emission because of the spatial resolution of 17 arcsec comparable to the spatial extent of the whole auroral region. The upper limit of the background disk emission is estimated from the total power when the northern aurora faces anti-earthward. The estimated value is ~150 GW, which is less than the total power ~450 GW when the auroral region faces earthward.

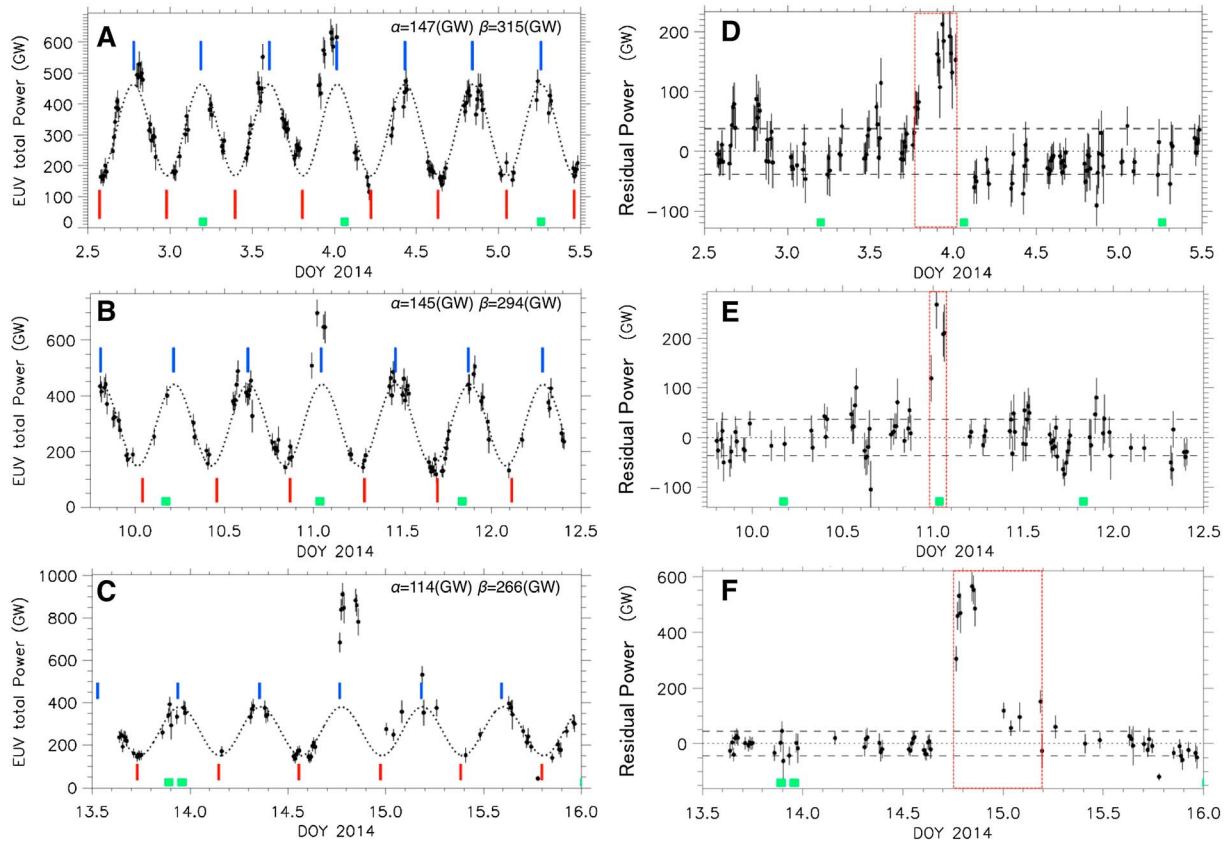

Figure 2. Time series of the sudden brightenings on days (a) 4, (b) 11, and (c) 14 of 2014 showing the total power of Jupiter's northern auroral emission at 900–1480 Å reduced from imaging spectra with 10 min integration time. The times when the northern aurora is facing the observer (Central Meridian Longitude, CML = 170°) are indicated by blue ticks, and the times when the northern aurora faces the opposite direction (CML = 350°) are indicated by red ticks. The times when northern auroral images were taken by HST/STIS are indicated by green ticks. The rotational modulation is estimated as a sinusoidal function $P = \alpha\, sin(2\pi\, f_{rot} t + \phi) + \beta$ with frequency of a planetary rotation f_{rot}, time t, arbitrary initial phase ϕ, amplitude α, and offset β. This function is fitted to data (dotted line) with a period of 9.925 h (Jupiter's rotation period), i.e., f_{rot} = 1/9.925 (1/h), with ϕ and β as free parameters. The time series during the sudden brightening (around day 3.9, 11.0, and 14.8) are ignored for the sinusoidal fitting. (d–f) The residuals from the sinusoidal function. The average and standard deviation of the residuals are indicated by dotted and broken lines, respectively. Again, the time series during the sudden brightening are ignored for computation of the average and standard deviation. The red-framed intervals are the period when the brightness is above the standard deviation with a duration more than 2 h.

During the coordinated observation campaign with Hisaki, HST took images of hydrogen molecular auroral emissions at 1250–1700 Å with a 0.08 arcsec resolution with the FUV-MultiAnode Microchannel Array detector of the Space Telescope Imaging Spectrograph (STIS) using the SrF2 long-pass filter (observation ID: GO13035). Fourteen images of Jupiter's northern aurora were taken from 1 to 16 January 2014, while Hisaki continuously observed Jupiter's northern aurora and Io plasma torus. The HST images were reduced using the pipeline described by *Clarke et al.* [2009] and *Nichols et al.* [2009].

There was no solar wind monitor near Jupiter during the Hisaki/EXCEED observation. We estimate the solar wind variation at Jupiter using a one-dimensional magnetohydrodynamic (MHD) model by propagating the solar wind measured around Earth [*Tao et al.*, 2005].

3. Result

During the joint HST campaign on 1–16 January 2014, we observed a series of sudden brightenings and decays in the auroral total power on days 4, 11, and 14. Figure 2 indicates the time series of the sudden brightening measured by EXCEED. The error bar is estimated based on Poisson statistics of the auroral source counts with the disk background counts. In Figures 2a–2c, the total power of the auroral emission is modulated by the apparent motion of auroral structures corotating with Jupiter as seen from Earth. The apparent rotational modulation is estimated by fitting a sinusoidal function to the time series. The residuals

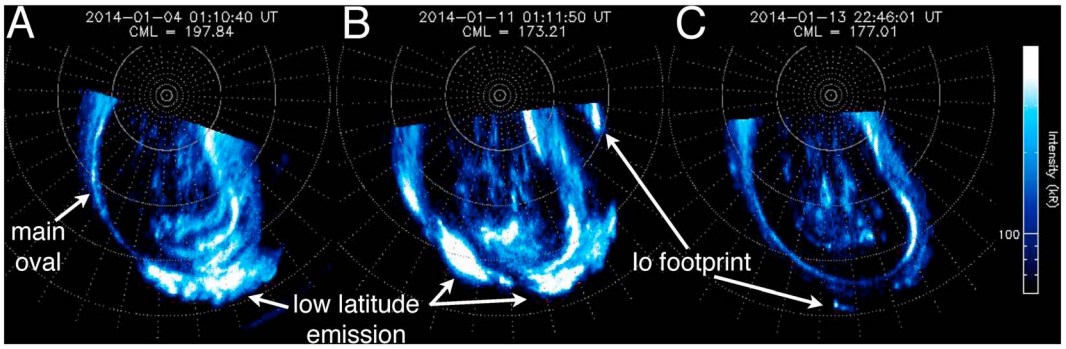

Figure 3. Polar projections of northern auroral emissions taken by HST/STIS with a spatial resolution of 0.08 arcsec (the pixel scale is 0.025 arcsec/pixel). (a) Image taken during the sudden brightening detected by Hisaki on day 4 2014. The projections are orientated with System III longitude = 180° at the bottom of each. The start time (not shifted for the light travel time from Jupiter) and CML of each image are labeled. (b) The auroral image taken on day 11 during the sudden brightening. HST could not image the sudden brightening on day 14. (c) An example auroral polar projection taken on day 13 when no sudden brightening was observed.

from the sinusoidal function are plotted in Figures 2d–2f. The total power of the sudden brightening reaches up to 210–550 GW in excess of the fitted sinusoid. These excess energies are 5–11 times larger than the standard deviations of the residuals. The duration of the sudden brightening is estimated based on the time when the excess energy is above the standard deviation for more than 2 h. The duration is constrained to be between 3 h and 11 h as indicated by the red-framed regions in Figures 2d–2f.

The high spatial resolution (0.08 arcsec) observations made by the STIS revealed the brightening of each auroral morphology around the sudden brightening seen in the total auroral power on days 4 and 11 as indicated by the green ticks in Figures 3a and 3b. On day 4, the auroral image was taken in the end of the sudden brightening. The low-latitude emission is expanded from the main oval down to latitudes around Io's footprint aurora. The emission is longitudinally localized with discrete structures. The power emitted from the low-latitude region at EUV to FUV wavelengths is estimated based on the method proposed by *Gustin et al*. [2012]. It is noticeably enhanced by ~100 GW above that during the surrounding observations (200 GW). On day 11, the auroral image was taken during the sudden brightening. The low-latitude emission and main oval are dominantly brightened simultaneously with a weak enhancement of the polar cap emission. The main oval and low-latitude emission are remarkably enhanced by ~700 GW and ~500 GW above those during the surrounding observations (200 and 300 GW), respectively. It should be noted that the total power determined from HST/STIS (from EUV to FUV) is larger than that from Hisaki by a factor of ~3 because of the different wavelength ranges covered. The bright blob of emission seen on the dawn flank of the HST image from day 11 is reminiscent of a dawn storm [*Clarke et al*., 2004]. However, it is located equatorward of the main oval and is much more compact than a dawn storm, which is a strong brightening of the morning arc of the main oval [e.g. *Gustin et al*., 2006]. On day 13, HST was taking an image much earlier than the sudden brightening. The HST observations made on the other days when sudden brightenings were not seen by Hisaki did not reveal any similar discrete low-latitude emissions. One example image taken when the total auroral power measured by Hisaki was close to the base value, as indicated by the dotted lines in Figure 2, is shown in Figure 3c.

The sudden brightenings occurred on days 4, 11, and 14 when the simulated solar wind was relatively quiet (Figure 4a). A forward shock, which is characterized by discontinuous increase in the solar wind dynamic pressure to 0.15 nPa and velocity to 450 km/s, was predicted to arrive at Jupiter on day 1–2 during the observing interval as indicated in Figures 4c and 4d. The uncertainty in the arrival time at Jupiter is estimated to be less than ±24 h, which corresponds to ~95% confidence interval, for day 1–17 when the Earth-Sun-Jupiter angle was less than 25° [*Tao et al*., 2005]. Thus, we assume that the sudden brightening on day 4 was not associated with the forward shock arrival. It should be noted that during the event on day 4 the dynamic pressure was estimated to be ~0.05 nPa, which corresponds to the trailing edge of the solar wind compression region. The dynamic pressure was 0.02 nPa during the event on day 11. Although this period is quieter than day 4, one should also note that a weak reverse shock, in which the dynamic pressure dropped slightly

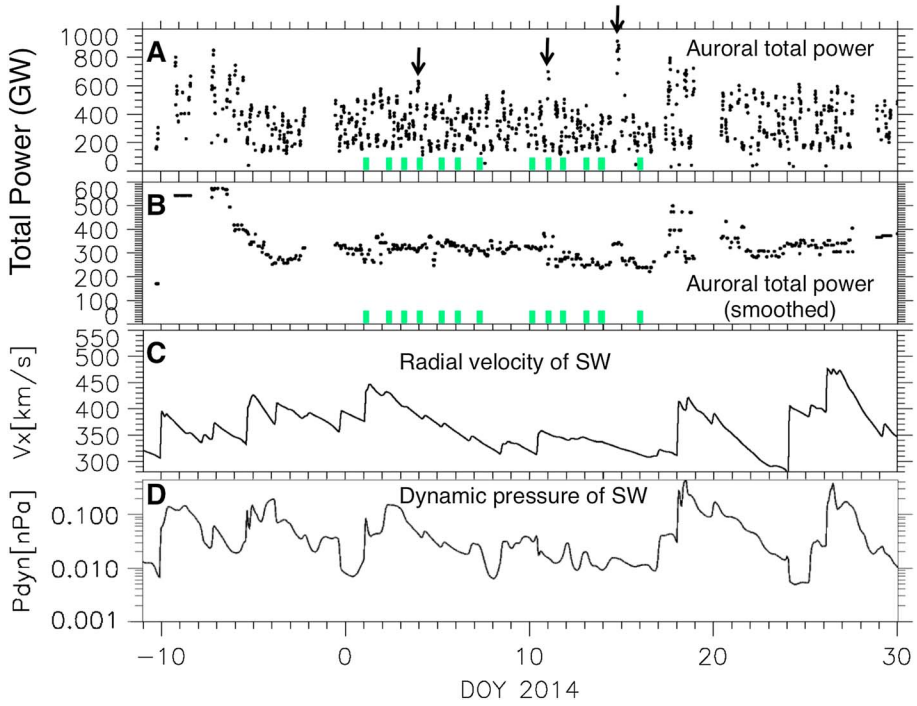

Figure 4. Total power of Jupiter's northern EUV aurora and solar wind parameters from day −10 to 30 2014 (from 21 December 2013 to 30 January 2014), including Jupiter's opposition seen from Earth on 6 January. (a) The auroral total power as a function of day 2014 (day 1 is equivalent to 1 January 2014). Vertical black arrows indicate days when the sudden brightening occurred on 4, 11, and 14. The times when northern auroral images were taken by HST/STIS are indicated by green ticks. (b) EUV auroral total power smoothed by running median with a window of four Jupiter's rotation periods (39.7 h). (c, d) Solar wind variations extrapolated from those observed at Earth to Jupiter based on magnetohydrodynamic (MHD) simulation [*Tao et al.*, 2005].

from 0.04 to 0.02 nPa, could have arrived at Jupiter during the event, followed by a rarefaction region. The rarefaction region continued with the pressure of 0.01 nPa during the event on day 14, which was separated by more than 2 days from any shock arrivals (on day 10.5 and 17). The power of 550 GW, which is the largest in the three events, was emitted on day 14 during this significant rarefaction region.

Enhancements in the auroral total power lasting a few days occurred in addition to the sudden brightening. Gradual variations around days −10 to −4 and 18 to 20 2014 accompany large interplanetary shocks in the simulated dynamic pressure and velocity after significant rarefaction regions (Figures 4a, 4c, and 4d). Their temporal evolution is clearly very different from the sudden brightenings, and they are particularly noticeable in the smoothed auroral power time series (Figure 4b). Based on the arrival time ambiguity of ±24 h, the gradual variations are interpreted as emissions driven externally by compression of the magnetosphere, as confirmed by previous HST auroral images [e.g., *Nichols et al.*, 2009; *Clarke et al.*, 2009]. The hourly continuous monitoring presented here resolves the solar wind-driven and nonsolar wind-driven (or modulated) auroral components for the first time, and shows that they occur independently of each other. From Figure 4b, the excess power of the solar wind-driven emissions on days −10 to −4 and 18 to 20 is estimated to be ~300 GW above the "quiet" emission level of 300 GW. This increase by a factor 2 is consistent with the previous HST observations [*Nichols et al.*, 2009; *Clarke et al.*, 2009], which indicated the increase in the auroral total power by a factor 2–4 during the solar wind compressions.

4. Discussion

The sudden brightening occurred with excess power of 210–550 GW preferably when the solar wind was relatively quiet. In particular, the largest power 550 GW was emitted during the significant rarefaction region. The excess power of 210–550 GW is comparable to the auroral power of ~300 GW during the following solar wind compression region. The observed auroral images suggest that the low-latitude emissions in the

postnoon sector, main oval accompanying the dawnside enhancement, and polar cap emission could have a contribution of 210–550 GW in total. Our continuous monitoring implies for the first time that the temporal evolution of these auroras is 3–11 h for this process.

The highly excess power of the sudden brightening suggests that substantial energy is rapidly supplied to the auroral emissions during the solar wind quiet period. The multiple auroral regions from the polar cap region down to low latitude around the latitudes of Io's footprint aurora are enhanced accompanying with this rapid energy supply. This implies a global change in any auroral particle precipitation processes: e.g., the rotationally driven auroral current driven in the middle magnetosphere [e.g., *Hill*, 2001], electron pitch angle scattering in the inner magnetosphere [*Mauk et al*., 2002; *Radioti et al*., 2009], and possibly auroral current driven by the dawnside tail reconnection [*Kasahara et al*., 2013].

It should be noted that this rapid energy supply is also feasible not only during the rarefaction region but also during the trailing edge of the weak solar wind compression and small reverse shock (see Figure 4). The event on day 4 during the trailing edge of the weak compression region may be associated with either a significant expansion of the magnetosphere or lie toward the end of an interval of enhanced open flux production that might precipitate enhanced nightside reconnection. The event on day 11 could involve the main oval enhancements during the solar wind expansion phase as suggested by *Cowley et al*. [2007].

The occurrence frequency of the sudden auroral brightening in this study is simply estimated as follows: three dominant (days 4, 11, and 14) events within a 2 week long interval, corresponding to a frequency of 1 event every 4.7 days. This is a comparable occurrence frequency to the auroral intensifications observed during the IUE monitoring campaign, which were observed every 4–10 days [*Prangé et al*., 2001].

Recurrent magnetospheric disturbances over a time scale of a few days have long been reported from previous observations. The particle energization in the tail region [*Woch et al*., 1998; *Krupp et al*., 1998; *Kronberg et al*., 2005, 2007, 2009], polar dawn spots [*Radioti et al*., 2008, 2011], radio emissions from the auroral region, and radio emissions from the Io plasma torus correlated with energetic particle injections [*Louarn et al*., 1998, 2000, 2007, 2014] were reported to occur at a frequency of 1.5–7 days. Based on Galileo's in situ and radio observations, *Louarn et al*. [2014] suggested that the global recurrent disturbance involves simultaneous auroral activation, formation of the radio emission source and particle injections in the Io torus, and magnetic reconfigurations and radial flow bursts in the distant disk over a time scale of a few hours. These studies suggested that the recurrent magnetospheric disturbances are related to the "Vasyliūnas cycle" [*Vasyliūnas*, 1983], which is a type of magnetospheric internal circulation on closed field lines driven by mass loading from the Io plasma torus, in which mass and energy are released via magnetic reconnection in the tail region of magnetosphere.

Cassini's observations of the Io plasma torus indicated the short-term variations in the sulfur ion line emissions, which is caused by the hot electron fraction increase in the torus, following the sudden auroral brightening [*Tsuchiya et al*., 2010]. This suggests that the hot plasma is transported radially inward, and/or plasma is locally heated by consuming energy transported after the sudden auroral brightening. The plasma torus heating simultaneously with the sudden auroral brightening supports their possible relationship to previously observed recurrent disturbances and the Vasyliūnas cycle [*Woch et al*., 1998; *Krupp et al*., 1998; *Louarn et al*., 1998, 2000, 2007, 2014; *Kronberg et al*., 2005, 2007, 2009].

Acknowledgments
This research was supported by a grant-in-aid for Scientific Research from the Japan Society for the Promotion of Science (JSPS). S.V.B. was supported by a Royal Astronomical Society Research Fellowship. This work is based on observations made with the NASA/ESA Hubble Space Telescope (observation ID: GO13035), obtained at the Space Telescope Science Institute, which is operated by AURA, Inc. for NASA. The data of Hisaki satellite are archived in the Data Archives and Transmission System (DARTS) JAXA.

The Editor thanks two anonymous reviewers for their assistance in evaluating this paper.

References

Baron, R. L., T. Owen, J. Connerney, T. Satoh, and J. Harrington (1996), Solar wind control of Jupiter's auroras, *Icarus*, *120*, 437–442, doi:10.1006/icar.1996.0063.

Bonfond, B., D. Grodent, J.-C. Gérard, T. Stallard, J. T. Clarke, M. Yoneda, A. Radioti, and J. Gustin (2012), Auroral evidence of Io's control over the magnetosphere of Jupiter, *Geophys. Res. Lett.*, *39*, L01105, doi:10.1029/2011GL050253.

Clarke, J. T., D. Grodent, S. Cowley, E. Bunce, J. Connerney, and T. Satoh (2004), Jupiter's aurora, in *Jupiter*, The Planet, Satellites and Magnetosphere, edited by F. Bagenal, T. E. Dowling, and W. B. McKinnon, pp. 639–670, Cambridge. Univ. Press, Cambridge, U. K.

Clarke, J. T., et al. (2009), Response of Jupiter's and Saturn's auroral activity to the solar wind, *J. Geophys. Res.*, *114*, A05210, doi:10.1029/2008JA013694.

Cowley, S. W. H., and E. J. Bunce (2003a), Modulation of Jovian middle magnetosphere currents and auroral precipitation by solar wind-induced compressions and expansions of the magnetosphere: Initial conditions and steady state, *Planet. Space Sci.*, *51*, 31–56, doi:10.1016/S0032-0633(02)00130-7.

Cowley, S. W. H., and E. J. Bunce (2003b), Modulation of Jupiter's main auroral oval emissions by solar wind induced expansions and compressions of the magnetosphere, *Planet. Space Sci.*, *51*, 57–79, doi:10.1016/S0032-0633(02)00118-6.

Cowley, S. W. H., J. D. Nichols, and D. J. Andrews (2007), Modulation of Jupiter's plasma flow, polar currents, and auroral precipitation by solar wind-induced compressions and expansions of the magnetosphere: A simple theoretical model, *Ann. Geophys.*, *25*, 1433–1463.
Grodent, D. (2014), A brief review of ultraviolet auroral emissions on giant planets, *Space Sci. Rev.*, doi:10.1007/s11214-014-0052-8.
Gurnett, D. A., et al. (2002), Control of Jupiter's radio emission and aurorae by the solar wind, *Nature*, *415*, 985–987, doi:10.1038/415985a.
Gustin, J., S. W. H. Cowley, J.-C. Gérard, G. R. Gladstone, D. Grodent, and J. T. Clarke (2006), Characteristics of Jovian morning bright FUV aurora from Hubble Space Telescope/Space Telescope Imaging Spectrograph imaging and spectral observations, *J. Geophys. Res.*, *111*, A09220, doi:10.1029/2006JA011730.
Gustin, J., B. Bonfond, D. Grodent, and J.-C. Gérard (2012), Conversion from HST ACS and STIS auroral counts into brightness, precipitated power, and radiated power for H_2 giant planets, *J. Geophys. Res.*, *117*, A07316, doi:10.1029/2012JA017607.
Hill, T. W. (2001), The Jovian auroral oval, *J. Geophys. Res.*, *106*, 8101–8107, doi:10.1029/2000JA000302.
Kasahara, S., E. A. Kronberg, T. Kimura, C. Tao, S. V. Badman, A. Masters, A. Retinò, N. Krupp, and M. Fujimoto (2013), Asymmetric distribution of reconnection jet fronts in the Jovian nightside magnetosphere, *J. Geophys. Res. Space Physics*, *118*, 375–384, doi:10.1029/2012JA018130.
Khurana, K. K., M. G. Kivelson, V. M. Vasyliūnas, N. Krupp, J. Woch, A. Lagg, B. H. Mauk, and W. S. Kurth (2004), The configuration of Jupiter's magnetosphere, in *Jupiter*, The Planet, Satellites and Magnetosphere, edited by F. Bagenal, T. E. Dowling, and W. B. McKinnon, pp. 593–616, Cambridge. Univ. Press, Cambridge, U. K.
Kronberg, E. A., J. Woch, N. Krupp, A. Lagg, K. K. Khurana, and K.-H. Glassmeier (2005), Mass release at Jupiter: Substorm-like processes in the Jovian magnetotail, *J. Geophys. Res.*, *110*, A03211, doi:10.1029/2004JA010777.
Kronberg, E. A., K.-H. Glassmeier, J. Woch, N. Krupp, A. Lagg, and M. K. Dougherty (2007), A possible intrinsic mechanism for the quasi-periodic dynamics of the Jovian magnetosphere, *J. Geophys. Res.*, *112*, A05203, doi:10.1029/2006JA011994.
Kronberg, E. A., J. Woch, N. Krupp, and A. Lagg (2009), A summary of observational records on periodicities above the rotational period in the Jovian magnetosphere, *Ann. Geophys.*, *27*, 2565–2573, doi:10.5194/angeo-27-2565-2009.
Krupp, N., J. Woch, A. Lagg, B. Wilken, S. Livi, and D. J. Williams (1998), Energetic particle bursts in the predawn Jovian magnetotail, *Geophys. Res. Lett.*, *25*, 1249–1252, doi:10.1029/98GL00863.
Krupp, N., et al. (2004), Dynamics of the Jovian magnetosphere, in *Jupiter*, The Planet, Satellites and Magnetosphere, edited by F. Bagenal, T. E. Dowling, and W. B. McKinnon, pp. 617–638, Cambridge. Univ. Press, Cambridge, U. K.
Louarn, P., A. Roux, S. Perraut, W. Kurth, and D. Gurnett (1998), A study of the large-scale dynamics of the Jovian magnetosphere using the Galileo plasma wave experiment, *Geophys. Res. Lett.*, *25*, 2905–2908, doi:10.1029/98GL01774.
Louarn, P., A. Roux, S. Perraut, W. S. Kurth, and D. A. Gurnett (2000), A study of the Jovian "energetic magnetospheric events" observed by Galileo: Role in the radial plasma transport, *J. Geophys. Res.*, *105*, 13,073–13,088, doi:10.1029/1999JA900478.
Louarn, P., et al. (2007), Observation of similar radio signatures at Saturn and Jupiter: Implications for the magnetospheric dynamics, *Geophys. Res. Lett.*, *34*, L20113, doi:10.1029/2007GL030368.
Louarn, P., C. P. Paranicas, and W. S. Kurth (2014), Global magnetodisk disturbances and energetic particle injections at Jupiter, *J. Geophys. Res. Space Physics*, *119*, 4495–4511, doi:10.1002/2014JA019846.
Mauk, B. H., J. T. Clarke, D. Grodent, J. H. Waite, C. P. Paranicas, and D. J. Williams (2002), Transient aurora on Jupiter from injections of magnetospheric electrons, *Nature*, *415*, 1003–1005, doi:10.1038/4151003a.
Nakaya, K., S. Fukuda, S. Sakai, A. Yamazaki, K. Uemizu, T. Toriumi, J. Takahashi, M. Maehara, T. Okahashi, and S. Sawai (2012), Trans. JSASS Aerospace Tech. Japan 10, Tf_5-Tf_9.
Nichols, J. D. (2011), Magnetosphere-ionosphere coupling in Jupiter's middle magnetosphere: Computations including a self-consistent current sheet magnetic field model, *J. Geophys. Res.*, *116*, A10232, doi:10.1029/2011JA016922.
Nichols, J. D., and S. W. H. Cowley (2003), Magnetosphere-ionosphere coupling currents in Jupiter's middle magnetosphere: Dependence on the effective ionospheric Pedersen conductivity and iogenic plasma mass outflow rate, *Ann. Geophys.*, *21*, 1419–1441.
Nichols, J. D., E. J. Bunce, J. T. Clarke, S. W. H. Cowley, J.-C. Gérard, D. Grodent, and W. R. Pryor (2007), Response of Jupiter's UV auroras to interplanetary conditions as observed by the Hubble Space Telescope during the Cassini flyby campaign, *J. Geophys. Res.*, *112*, A02203, doi:10.1029/2006JA012005.
Nichols, J. D., J. T. Clarke, J.-C. Gérard, D. Grodent, and K. C. Hansen (2009), Variation of different components of Jupiter's auroral emission, *J. Geophys. Res.*, *114*, A06210, doi:10.1029/2009JA014051.
Prangé, R., G. Chagnon, M. G. Kivelson, T. A. Livengood, and W. Kurth (2001), Temporal monitoring of Jupiter's auroral activity with IUE during the Galileo mission. Implications for magnetospheric processes, *Planet. Space Sci.*, *49*, 405–415, doi:10.1016/S0032-0633(00)00161-6.
Prangé, R., L. Pallier, K. C. Hansen, R. Howard, A. Vourlidas, R. Courtin, and C. Parkinson (2004), An interplanetary shock traced by planetary auroral storms from the Sun to Saturn, *Nature*, *432*, 78–81, doi:10.1038/nature02986.
Pryor, W. R., et al. (2005), Cassini UVIS observations of Jupiter' auroral variability, *Icarus*, *178*, 312–326, doi:10.1016/j.icarus.2005.05.021.
Radioti, A., D. Grodent, J.-C. Ge´rard, B. Bonfond, and J. T. Clarke (2008), Auroral polar dawn spots: Signatures of internally driven reconnection processes at Jupiter's magnetotail, *Geophys. Res. Lett.*, *35*, L03104, doi:10.1029/2007GL032460.
Radioti, A., A. T. Tomás, D. Grodent, J.-C. Gérard, J. Gustin, B. Bonfond, N. Krupp, J. Woch, and J. D. Menietti (2009), Equatorward diffuse auroral emissions at Jupiter: Simultaneous HST and Galileo observations, *Geophys. Res. Lett.*, *36*, L07101, doi:10.1029/2009GL037857.
Radioti, A., D. Grodent, J. C. Gérard, M. F. Vogt, M. Lystrup, and B. Bonfond (2011), Nightside reconnection at Jupiter: Auroral and magnetic field observations from 26 July 1998, *J. Geophys. Res.*, *116*, A03221, doi:10.1029/2010JA016200.
Tao, C., R. Kataoka, H. Fukunishi, Y. Takahashi, and T. Yokoyama (2005), Magnetic field variations in the Jovian magnetotail induced by solar wind dynamic pressure enhancements, *J. Geophys. Res.*, *110*, A11208, doi:10.1029/2004JA010959.
Tsuchiya, F., et al. (2010), Plan for observing magnetospheres of outer planets by using the EUV spectrograph onboard the SPRINT-A/EXCEED mission, *Adv. Geosci.*, *25*, 57–71, doi:10.1142/9789814355377_0005.
Vasyliūnas, V. M. (1983), Plasma distribution and flow, in *Physics of the Jovian Magnetosphere*, edited by A. J. Dessler, pp. 395–453, Cambridge Univ. Press, New York.
Waite, J. H., Jr., et al. (2001), An auroral flare at Jupiter, *Nature*, *410*, 787–789, doi:10.1038/35071018.
Woch, J., N. Krupp, A. Lagg, B. Wilken, S. Livi, and D. J. Williams (1998), Quasi-periodic modulations of the Jovian magnetotail, *Geophys. Res. Lett.*, *25*, 1253–1256, doi:10.1029/98GL00861.
Yates, J. N., N. Achilleos, and P. Guio (2014), Response of the Jovian thermosphere to a transient 'pulse' in solar wind pressure, *Planet. Space Sci.*, *91*, 27–44, doi:10.1016/j.pss.2013.11.009.
Yoneda, M., F. Tsuchiya, H. Misawa, B. Bonfond, C. Tao, M. Kagitani, and S. Okano (2013), Io's volcanism controls Jupiter's radio emissions, *Geophys. Res. Lett.*, *40*, 671–675, doi:10.1002/grl.50095.
Yoshioka, K., G. Murakami, A. Yamazaki, F. Tsuchiya, M. Kagitani, T. Sakanoi, T. Kimura, K. Uemizu, K. Uji, and I. Yoshikawa (2013), The extreme ultraviolet spectroscope for planetary science, EXCEED, *Planet. Space Sci.*, *85*, 250–260, doi:10.1016/j.pss.2013.06.021.